AFRL-PR-WP-TP-2006-227

PINNING ENHANCEMENT OF $YBa_2Cu_2O_{7-d}$ THIN FILMS WITH Y_2BaCuO_5 PARTICULATES

Paul N. Barnes, Timothy J. Haugan, Michael D. Sumption, and B. Craig Harrison

OCTOBER 2004

Approved for public release; distribution is unlimited.

STINFO COPY

PROPULSION DIRECTORATE
AIR FORCE MATERIEL COMMAND
AIR FORCE RESEARCH LABORATORY
WRIGHT-PATTERSON AIR FORCE BASE, OH 45433-7251

REPORT DOCUMENTATION PAGE

Form Approved
OMB No. 0704-0188

1. REPORT DATE *(DD-MM-YY)*	2. REPORT TYPE	3. DATES COVERED *(From - To)*
October 2004	Journal Article Postprint	11/05/2003 – 10/05/2004

4. TITLE AND SUBTITLE
PINNING ENHANCEMENT OF $YBa_2Cu_2O_{7-d}$ THIN FILMS WITH Y_2BaCuO_5 NANOPARTICULATES

5a. CONTRACT NUMBER
In-house

5b. GRANT NUMBER

5c. PROGRAM ELEMENT NUMBER
61102F/62203F

6. AUTHOR(S)
Paul N. Barnes, Timothy J. Haugan, Michael D. Sumption, and B. Craig Harrison

5d. PROJECT NUMBER
3145

5e. TASK NUMBER
32

5f. WORK UNIT NUMBER
31453279

7. PERFORMING ORGANIZATION NAME(S) AND ADDRESS(ES)
Power Generation Branch (AFRL/PRPG)
Power Division
Propulsion Directorate
Air Force Research Laboratory, Air Force Materiel Command
Wright-Patterson Air Force Base, OH 45433-7251

8. PERFORMING ORGANIZATION REPORT NUMBER
AFRL-PR-WP-TP-2006-227

9. SPONSORING/MONITORING AGENCY NAME(S) AND ADDRESS(ES)
Propulsion Directorate
Air Force Research Laboratory
Air Force Materiel Command
Wright-Patterson AFB, OH 45433-7251

10. SPONSORING/MONITORING AGENCY ACRONYM(S)
AFRL-PR-WP

11. SPONSORING/MONITORING AGENCY REPORT NUMBER(S)
AFRL-PR-WP-TP-2006-227

12. DISTRIBUTION/AVAILABILITY STATEMENT
Approved for public release; distribution is unlimited.

13. SUPPLEMENTARY NOTES
Journal article postprint published in IEEE Transactions on Applied Superconductivity, Vol. 15, No. 2, June 2005.

PAO case number: ASC 04-0966; Date cleared: 07 Apr 2004.

14. ABSTRACT
A comparison study is given of a typical superconducting $YBa_2Cu_3O_{7-d}$ (Y123) film and a Y123 film containing a nonsuperconducting Y_2BaCuO_5 (Y211) phase nanoparticulate dispersion. The inclusion of the second phase nanoparticulates was for the express purpose of increasing superconducting film's magnetic pinning strength with the resultant improved in-field critical current density. $LaAlO_3$ substrates were used and the Y123 and Y211 nanoparticulates were grown by pulsed laser deposition (PLD). The Y211 nanoparticulate dispersion in the Y123 resulted from multiple consecutive depositions by PLD of the respective targets. The Y123 phase maintained excellent epitaxy with high in-plane orientation with and without the Y211 inclusions. With the Y211 additions, the critical current densities of the films increased significantly in applied magnetic fields as compared to the high quality Y123 film with no Y211 additions.

15. SUBJECT TERMS
Flux Pinning, nanoparticulates, YBCO, Y_2BaCuO_5

16. SECURITY CLASSIFICATION OF:			17. LIMITATION OF ABSTRACT:	18. NUMBER OF PAGES	19a. NAME OF RESPONSIBLE PERSON (Monitor)
a. REPORT	b. ABSTRACT	c. THIS PAGE			Paul N. Barnes
Unclassified	Unclassified	Unclassified	SAR	10	19b. TELEPHONE NUMBER *(Include Area Code)* N/A

Pinning Enhancement of $YBa_2Cu_3O_{7-d}$ Thin Films With Y_2BaCuO_5 Nanoparticulates

Paul N. Barnes, Timothy J. Haugan, Michael D. Sumption, and B. Craig Harrison

***Abstract*—A comparison study is given of a typical superconducting $YBa_2Cu_3O_{7-d}$ (Y123) film and a Y123 film containing a nonsuperconducting Y_2BaCuO_5 (Y211) phase nanoparticulate dispersion. The inclusion of the second phase nanoparticulates was for the express purpose of increasing superconducting film's magnetic pinning strength with the resultant improved in-field critical current density. $LaAlO_3$ substrates were used and the Y123 and Y211 nanoparticulates were grown by pulsed laser deposition (PLD). The Y211 nanoparticulate dispersion in the Y123 resulted from multiple consecutive depositions by PLD of the respective targets. The Y123 phase maintained excellent epitaxy with high in-plane orientation with and without the Y211 inclusions. With the Y211 additions, the critical current densities of the films increased significantly in applied magnetic fields as compared to the high quality Y123 film with no Y211 additions.**

***Index Terms*—Flux Pinning, nanoparticulates, YBCO, Y_2BaCuO_5.**

I. Introduction

HIGH TEMPERATURE superconducting (HTS) $YBa_2Cu_3O_{7-d}$ (YBCO or Y123) superconductors are being developed for a variety of applications since high critical current densities (J_c) are maintained in applied magnetic fields of a few tesla. Because of this, YBCO coated conductors are considered the second generation HTS wire to the first generation $Bi_2Sr_2Ca_2Cu_3O_8$ (BSCCO). The primary uses for HTS wire are in power applications such as transformers, generators, motors, power transmission cables, etc [1], [2]. Even though YBCO has good in-field properties at 77 K, it is of interest to further enhance its performance by improving the flux pinning characteristics of the superconductor. This is especially true since J_c can decline by an order of magnitude at 1 T magnetic fields applied in the c-axis direction of YBCO [3], [4]. An increase of the critical current in the superconducting film can lead to a higher engineering current density for the HTS wire, the more critical wire parameter [5].

The mechanisms of flux pinning typically occurring in YBCO films grown on varying substrates (or buffered substrates) is not immediately evident since the coherence length in this superconductor is quite small, $\xi \sim 1.5$–2 nm [1]. Because of the small coherence length, a variety of atomic size structures or defects in the film can pin the fluxons. However, this does suggest that a high density of nanosized particulates dispersed throughout the superconductor can be an effective pinning structure as opposed to only columnar defects effectively pinning the magnetic vortices [1], [6] if the particulate dispersion is sufficiently dense.

Y_2BaCuO_5 (Y211) has previously been used to confer pinning in bulk YBCO superconductors, but this has been principally in melt textured and bulk material [7]–[11]. In these cases, the size of the Y211 inclusions were typically on the order of a micron in size and particle density was low resulting in mediocre pinning at best. If an effective way of introducing Y211 into Y123 can be devised, Y211 has several advantages to be used as a material for the incorporation of pinning centers into Y123. Y211 is chemically stable with Y123 resulting in little if any chemical diffusion or reaction [12]. Also, deposition conditions for Y211 growth are quite similar to Y123 making in-situ growth of Y211 particulates easier to accomplish.

Recently, a method has been reported by T. J. Haugan *et al.* to incorporate Y211 sites into Y123 as a nanoparticulate dispersion using pulsed laser deposition [13], [14]. Alternating depositions of Y211 and Y123 were performed in very short intervals to accomplish this. Due to the lattice mismatch between Y211 and Y123 the Y211 formed islands of several nanometers in size during growth. A subsequent deposition of the Y123 on top of the Y211 particles dispersed on the Y123 layer resulted in epitaxial growth of the Y123 on the exposed parts of the Y123 surface. The process was continuously repeated to provide the desired thickness of the composite film. Use of a nonlattice matched material represents a different approach for the use of multilayer deposition which focused on island growth. This paper uses the same procedure described in that report to compare the pinning force associated with the Y123/Y211 film to a typical YBCO film. A comparison of magnetic J_c and the pinning force density of a plain Y123 sample and a Y211/123 composite sample is given.

II. Experimental Details

Samples were prepared by pulsed laser deposition, and two samples representative of the group, either plain YBCO films or composite Y211/Y123 films, were used for comparison. One sample, a control sample identified as TJ360, consisted of a typical YBCO film deposited on single crystal $LaAlO_3$ (LAO). The second sample, TJ127C, consisted of YBCO with a Y211 nanoparticulate inclusion, also identified as $(Y211_{1.6\ nm}/Y123_{6.1\ nm}) \times 35$. The alternate layers of the Y211 nanoparticulate and the Y123 were deposited using conditions reported previously [13], [14]. The amount of material deposited in the Y123/Y211 nanoparticulate bilayer was

Manuscript received October 5, 2004. This work supported by the U.S. Air Force Office of Scientific Research and Air Force Research Laboratory.

P. N. Barnes, T. J. Haugan, and B. C. Harrison are with the Air Force Research Laboratory, Wright-Patterson AFB, OH 45433 USA (e-mail: paul.barnes@wpafb.af.mil; timothy.haugan@wpafb.af.mil).

M. D. Sumption is a Summer Faculty with the Air Force Research Laboratory, Wright-Patterson AFB, OH 45433 USA, from the Ohio State University, Columbus, OH 43210 USA (e-mail: mdsumption+@osu.edu).

Digital Object Identifier 10.1109/TASC.2005.849426

such that if deposited separately and uniformly, the Y123 layer would be 6.1 nm thick and the Y211 layer would be 1.6 nm thick. However, deposition of the Y211 on the Y123 layer resulted in a dispersive growth of Y211 nanoparticulates.

It is not clear if the entire Y211 deposition resulted in Y211 growth only. It is possible that there was some epitaxial Y123 growth during the Y211 deposition since Y, Ba Cu, and O (in one form or another) were all present in the laser ablation plume and the existing Y123 layer may initially favor Y123 growth, which would later give way to Y211 growth due to the ratio of elements present in the plume. Even so, x-ray data clearly indicate the presence of Y211 in the composite films. Results also substantiate growth of the Y211 was caused by lattice mismatching with the Y123 achieving a Y211 particle size of ~10–20 nm in diameter and ~4 nm in height. The sequential PLD depositions were automated with the laser pulses trigger-actuated by computer control. Film growth was stopped between each layer while the other target was rotated into position.

A Lambda Physik laser, model LPX 305i, was used at 248 nm, the KrF wavelength, pulsing at a 4 Hz rate. The ablation spot size was $\sim$ 6.5 mm^2 with a laser fluence of $\sim$ 3.2 $\mathrm{J/cm}^2$. The oxygen deposition pressure was 300 mTorr kept constant by downstream flow control while an O_2 gas (99.999% purity) flow of ~1 l/min was introduced during growth. The deposition targets were rotated and rastered radially during deposition for uniform target wear. Single crystal substrates of LAO were ultrasonically cleaned for 2 minutes prior to use. A thin layer of colloidal Ag paint was used to attach samples to the heater. Substrates sizes were approximately $3.2 \times 3.2\ \mathrm{mm}^2$. YBCO thickness was ~300 nm total thickness for each of the films.

After deposition, films were cooled from 785°C to 750°C,< 2 min, after which the vacuum pumps and O_2 pressure control were halted. The O_2 flow rate was increased to ~1.5 l/min into the chamber and the films cooled from 750°C to 500°C over a span of ~12 min. The deposited films were then held at 500°C for 30 minutes and the O_2 pressure was increased to 1 atm. The films were finally cooled from 500°C to room temperature prior to removal. This cooling process allows for oxygenation of the films.

Transport critical current densities (J_c) were acquired by the 4-point contact method using pogo pins for current contacts and a 1 $\mu\mathrm{V/cm}$ criterion. On these samples, the current and voltage contacts for the resistive measurement were patterned onto the films by DC magnetron sputter deposition of Ag with $\sim 3\ \mu\mathrm{m}$ thickness. The contact resistance of the Ag contacts on the YBCO films was reduced by annealing in pure O_2. To determine the pinning force, samples were mounted in a vibrating sample magnetometer (VSM). The samples were mounted such that the field was applied perpendicular to the wide face of the sample with currents induced in the $a-b$ planes of the HTS films. M-H loops were obtained in 10 minute collection periods at several temperatures ranging from 10 K to 77 K, with varying ramp rates. Temperatures were determined by a Si-diode placed near sample. The resulting M-H loops were volume normalized and then the magnetic J_c was extracted via $J_c = 30 \cdot \Delta M/d$ (here we use 20 rather than 30 as the prefactor to account for a finite size sample with $d = L$).

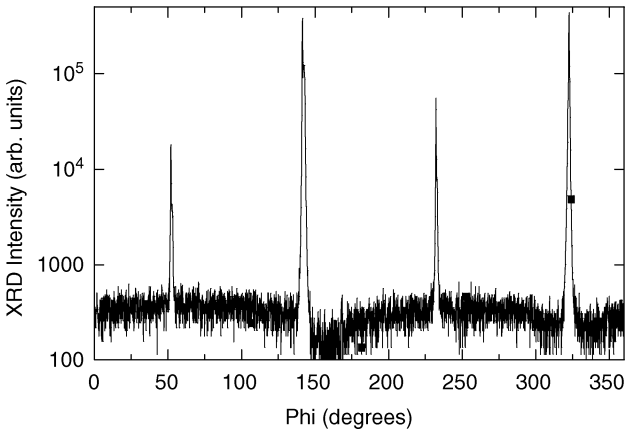

Fig. 1. Typical phi scan of the (103) peak for the Y123/Y211 (sample TJ127C) indicating the Y123 phase maintained excellent ab in-plane alignment with the Y211 nanoparticulate additions.

The superconducting transition temperature (T_c) was measured using an AC susceptibility technique with the amplitude of the magnetic sensing field varied from 0.025 Oe to 2.2 Oe, at a frequency of approximately 4 kHz. The T_c measurements were accurate within $\leq$ 0.1 K at three calibration points: liquid He at 4.2 K, liquid N_2 at 77.2 K, and room temperature. X-ray diffraction $\theta-2\theta$ scans were made with a Rigaku diffractometer, with a 2θ step-size of 0.03 Å and a count time of 1.8 s.

III. Results and Discussion

In general, the composite films displayed a sharp transition at T_c, as does the plain Y123 films, indicating good quality as determined by ac susceptibility measurements for a YBCO and Y211/Y123 composite film representative of the deposition group. A slight depression of T_c occurred for the composite films of a couple degrees. Transport measurement of the self-field J_c, at 77 K, for representative samples indicated that both YBCO and the composite films were between $\sim 2{-}3\ \mathrm{MA/cm}^2$. The Phi scan shown in Fig. 1 of the Y123/Y211 composite film, TJ127C, indicates that the Y123 phase maintained excellent ab in-plane alignment even with the Y211 nanoparticulate additions. In one case, the deposition was halted immediately after a Y211 deposition for imaging by scanning electron microscopy (SEM). The image is shown in Fig. 2. The Y211 nanoparticles are clearly visible on the surface of the Y123 phase material. The 2-θ scans confirm the presence of the Y211 phase growth.

A comparison of magnetic J_c values for the YBCO and the Y123/Y211 composite film are given in Fig. 3. This figure provides the relative change in J_c between the composite Y123/Y211 films and the plain Y123 films bearing in mind that transport J_c measurements confirm the over $\mathrm{MA/cm}^2$ performance of films as previously mentioned. Temperatures ranged from 10–77 K in 10 degree increments. Note that for these two particular samples the J_cs of the composite film increased from ~2 times to ~3 times in value at 1 T over the YBCO sample for the given temperature range. Values at low temperatures are significantly greater for the Y211/123 composite film over YBCO reference sample. This clearly demonstrates that flux

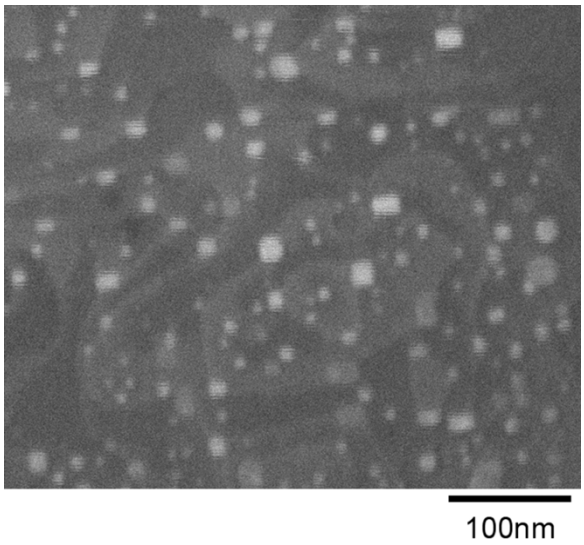

Fig. 2. SEM of localized area of a Y123/Y211 composite sample after halting growth following the Y211 deposition. The Y211 particulates are visible on the surface.

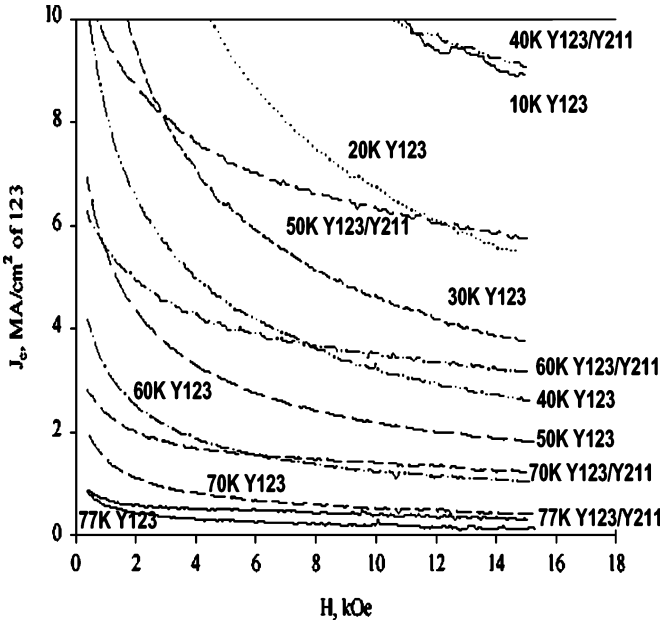

Fig. 3. In-field magnetic J_c for Y123 and Y123/Y211 samples at higher temperatures.

pinning advantages are conferred by the Y211 nanoparticulate inclusions.

The next two figures, Figs. 4, 5, show this in terms of the pinning force curves where $F_p = J_c \cdot B$, where the force is in $\mathrm{GN/m^3}$. This further demonstrates that the addition of Y211 nanoparticulate inclusions significantly enhances YBCO thin film performance. This is different then previous attempts at Y211 inclusion in Y123 phase material when limited benefit was observed [7]–[11]. The primary difference here is the small nanosize scale of the particles and the high density number. This indicates that significant pinning can be accomplished with nanoparticulates as with columnar defects. An advantage of the nanoparticulates is that directionality of the applied fields is less relevant as in the case of the oriented columnar defects.

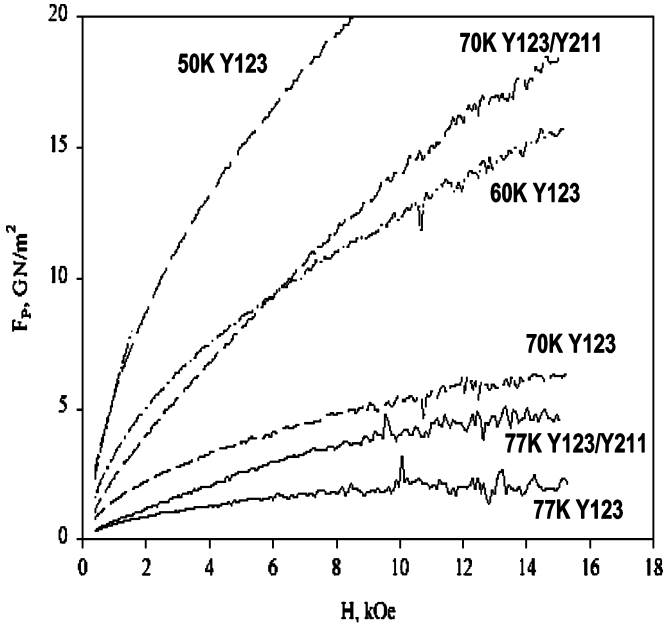

Fig. 4. Fp vs. H curves for Y123 (sample TJ360) and Y123/Y211 (sample TJ127C) at the higher temperatures for the 10–77 K temperature range considered.

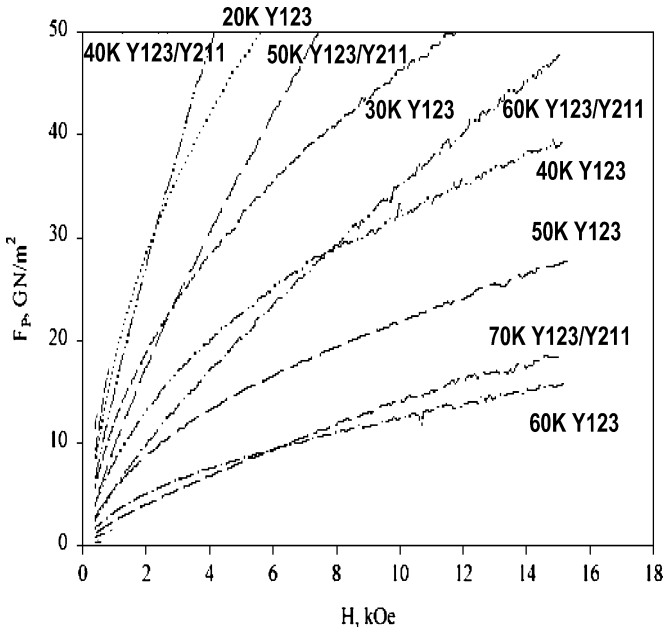

Fig. 5. Fp vs. H curves for Y123 (sample TJ360) and Y123/Y211 (sample TJ127C) at intermediate temperatures for the 10–77 K temperature range considered.

The matching field in the c-axis direction should correlate to the given density of the nanoparticles. Based on similarly prepared samples, this is at a magnetic field greater than the data assembled here but is not sufficiently clear for a definitive comparison at the present. However, for the magnetic field in the a-b plane direction, the matching field clearly corresponds to the spacing of the Y211 nanoparticulate planes [15]. Additional data is being collected to examine these issues as well as the relevant angular dependence of these films.

IV. Conclusion

The composite films consisting of essentially Y123 material with a naoparticulate dispersion of Y211 second phase addition achieved a high inclusion density resulting in significant pinning of YBCO. Addition of the Y211 nanoparticles had a negligible effect on c-axis and ab in-plane orientation of the Y123 phase. In the composite Y123/Y211 films, the critical current densities increased 2–3 times over that of the YBCO control sample for applied magnetic fields of 1 T from 10 K to 77 K. This demonstrates the effectiveness of high density nanoparticle dispersions in HTS films for magnetic flux pinning.

Acknowledgment

The authors thank Dr. I. Maartense for the ac susceptibility measurement performed for the samples and J. Evans for the x-ray diffraction measurements.

References

[1] D. Larbalestier, A. Gurevich, M. Feldman, and A. Polyanskii, *Nature*, vol. 414, p. 368, 2001.

[2] P. N. Barnes, G. L. Rhoads, J. C. Tolliver, M. D. Sumption, and K. W. Schmaeman, "Compact, lightweight superconducting power generators," presented at the 12th Symp. Electromagn. Launch Technol., 2004.

[3] S. R. Foltyn, E. J. Peterson, J. Y. Coulter, P. N. Arendt, Q. X. Jia, P. C. Dowden, M. P. Maley, X. D. Wu, and D. E. Peterson, *J. Mater. Res.*, vol. 12, p. 2941, 1997.

[4] T. Aytug, M. Paranthaman, S. Sathyamurthy, B. W. Kang, D. B. Beach, E. D. Specht, D. F. Lee, R. Feenstra, A. Goyal, D. M. Kroeger, K. J. Leonard, P. M. Martin, and D. K. Christen, Reel-to-reel continous chemical solution deposition of epitaxial Gd_2O_3 buffer layers on biaxial textured for the fabrication of $YBa_2Cu_3O_{7-d}$ coated conductors, in ORNL Superconducting Technology Program for Electric Power Systems, Annu. Rep. FY 2001, pp. 1-25–1-34.

[5] G. N. Riley, Q. Li, and L. G. Fritzmeier, *Current Opin. Solid State Mat. Sci.*, vol. 4, p. 473, 1999.

[6] T. Matsushita, *Supercond. Sci. Technol.*, vol. 13, p. 730, 2000.

[7] M. Murakami, S. Gotoh, H. Fujimoto, K. Yamaguchi, N. Koshizuka, and S. Tanaka, *Supercond. Sci. Technol.*, vol. 4, p. S43, 1991.

[8] S. Jin, G. W. Kamlott, T. H. Tiefel, T. Kodas, T. L. Ward, and D. M. Kroeger, *Phys. C*, vol. 181, p. 57, 1992.

[9] D. Shi, S. Sengupta, J. S. Luo, C. Varanasi, and P. J. McGinn, *Phys. C*, vol. 213, p. 179, 1993.

[10] M. Chopra, S. W. Chan, R. L. Meng, and C. W. Chu, *J. Mater. Res.*, vol. 11, p. 1616, 1996.

[11] S. Sengupta, D. Shi, J. S. Luo, A. Buzdin, V. Gorin, V. R. Todt, C. Varanasi, and P. J. McGinn, *J. Appl. Phys.*, vol. 81, p. 7396, 1997.

[12] J. D. Whitler and R. S. Roth, Eds., *Phase Diagrams for High Tc Superconductors*. Westerville, OH: American Ceramic Society, 1991.

[13] T. J. Haugan, P. N. Barnes, I. Maartense, E. J. Lee, M. D. Sumption, and C. B. Cobb, *J. Mater. Res.*, vol. 18, p. 2618, 2003.

[14] T. Haugan, P. N. Barnes, R. Wheeler, F. Meisenkothen, and M. Sumption, *Nature*, vol. 430, p. 867, 2004.

[15] L. Civale, Los Alamos National Laboratory, based on analysis of similar samples, private communication.